Microreactors

Bubble Microreactors Triggered by an Alternating Magnetic Field as Diagnostic and Therapeutic Delivery Devices**

Fang Yang, Ping Chen, Wen He, Ning Gu, Xizhi Zhang, Kun Fang, Yu Zhang, JianFei Sun, and Jiayi Tong*

Advances in the medical treatment of a wide variety of pathophysiological conditions require the development of better therapeutic agents, as well as a combination of the required therapeutic agents with diagnostic-integrated devices. With the development of micro- and nanotechnologies, the better intelligent medical systems and devices have profoundly impacted medical theranostic techniques.[1] Based on multifunctional device platforms, the interests of these studies mainly focus on multimodal imaging and simultaneous therapy, which provide patients with imaging (ultrasound, computed tomography, magnetic resonance imaging (MRI), etc.) and effective therapeutic agents responding directly at the disease sites.[2]

In recent years, micro- and nanoscale intelligent systems have become a desirable method to maximize the efficacy of therapeutic treatments in numerous ways, because they can release their contents in a ''smart or intelligent'' way by responding to external triggers or biomarkers.[3] These delivery vehicles include polymeric micelles, gels, liposomes, small colloidal particles, and nanoengineered polymeric or polyelectrolyte multilayered microcapsules.[4] Among them, microcapsules or microcontainers can serve as sensors or effective carriers for the delivery of encapsulated compounds.[5] The drugs or other macromolecular bioactives can be entrapped in the inner volume of the microcontainers, the shells of which can prevent any contact of the drug with healthy tissue before reaching the disease sites or specific tissues. To exhibit relatively large and sharp physical–chemical changes in response to small physical or chemical stimuli at the specific site, the shell materials can be deliberately chosen or modified.[6] Thus, these fabricated microstructures may offer a unique opportunity to combine surface multifunctionality with design flexibility for the delivery of encapsulated materials into designated target sites. However, it is a challenge to elaborate the successful operation of a whole delivery system possessing both medical imaging functionalities and controlled release properties. Externally triggered release has recently been shown to be a promising pathway. Such intelligent delivery systems can be classified into two types. First, systems responsive to external physical stimuli, such as microwave, acoustic, laser light, electric field, and magnetic treatment.[7–9] Second, in vivo systems responsive to chemical stimuli, such as temperature, Ca^{2+} or K^{+} ions, and pH variation.[10,11]

Magnetic fields have been used extensively in biomedical applications to allow the remote management of drug release from magnetic drug carriers, MRI, or hyperthermia therapy.[12–16] Herein, we investigate the possibility of using alternating magnetic field treatment as a remote trigger for the release of materials encapsulated in multilayer microcontainers. L-Arginine, a nitric oxide (NO) precursor agent,[17] was encapsulated in the core of microcontainers. It can be reduced by H_2O_2 or NO synthase in virtually all mammalian cells and tissues, including adipocytes, brain, endothelial cells, heart, hepatocytes, macrophages, and skeletal muscle.[18,19] The polymer double-layer shells were doped with superparamagnetic Fe_3O_4 nanoparticles, which can be manipulated by an external magnetic force. Under magnetic field exposure, the encapsulated Fe_3O_4 nanoparticles in the shell induce a change between ''open'' and ''closed'' states, which allows exchange of the arginine solution inside and H_2O_2 solution outside the microcontainers. Once the arginine makes contact with H_2O_2, NO gas can be continuously produced in the microcontainers. The microcontainers can thus be viewed as ''microreactors'' for synthesis of the interior NO gas.

[*] Prof. N. Gu, Dr. F. Yang, P. Chen, W. He, X. Zhang, K. Fang, Prof. Y. Zhang, J. F. Sun
School of Biological Science and Medical Engineering
Southeast University
Nanjing 210096 (P.R. China)
and
Jiangsu Key Laboratory for Biomaterials and Devices
Nanjing 210009 (P.R. China)
and
State Key Laboratory of Bioelectronics
Nanjing 210096 (P.R. China)
E-mail: guning@seu.edu.cn
Dr. J. Tong
Department of Cardiology
Zhongda Hospital
Southeast University
Nanjing 210009 (P.R. China)

[**] This investigation was financially supported by the National Important Science Research Program of China (Nos. 2006CB933206, 2006CB705606) and the National Natural Science Foundation of China (Nos. 60725101, 50872021, 30970787).

DOI: 10.1002/smll.201000173

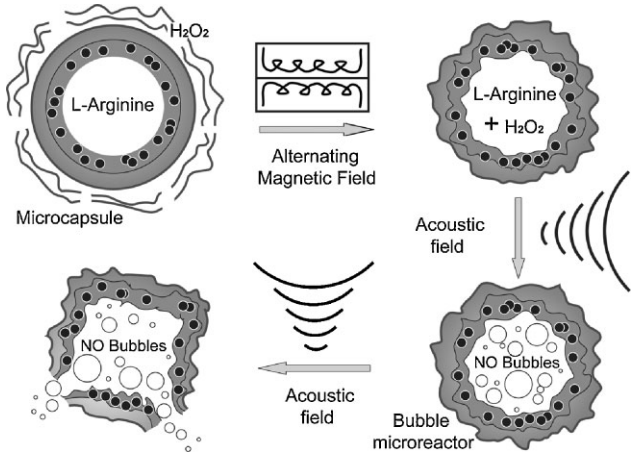

Figure 1. Schematic representation of the microcontainer with encapsulated L-arginine and Fe_3O_4 nanoparticles, which turns into a NO bubble microreactor as a result of an alternating magnetic field triggering controlled release. Shell permeability and rupture emerge upon treatment with the alternating magnetic field and US field exposure.

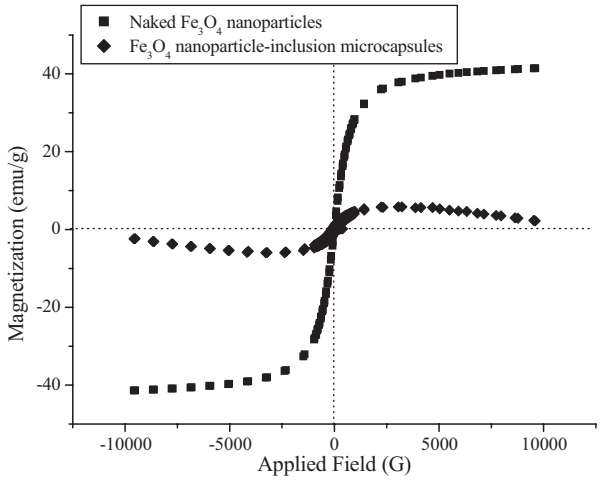

Figure 3. Magnetization curves of naked Fe_3O_4 nanoparticles and Fe_3O_4-inclusion microcapsules at room temperature.

The gas generated inside the bubble microreactors can be used as an ultrasound contrast agent (UCA) to enhance the contrast effect of ultrasound (US) imaging, because the NO bubbles allow the microcontainers to be efficient scatterers of US.[20] When these acoustic microreactors are further subjected to successive US exposure, the continuous bubble-based stable cavitation or noninertial ultrasonic cavitation may finally distort the shell integrity, even at low input power, and further release the interior components.[21] The proposed microcontainer design is illustrated in Figure 1, which shows schematically that the bubble microreactor triggered by an alternating magnetic field can be a good candidate for diagnostic and therapeutic delivery devices.

The microcontainers were fabricated using the double-emulsion method. The microscopy image in Figure 2a indicates the regular spherical morphology of the microcontainers. The mean diameter of the prepared microcontainers (each sample in triplicate) was found to be about 7.26 μm with a slightly asymmetric distribution, as shown in Figure 2b.

The magnetic properties of the microcontainers were investigated at room temperature. Figure 3 shows the magnetic hysteresis curves of the naked Fe_3O_4 nanoparticles and Fe_3O_4 nanoparticle-inclusion microcontainers. There is no remanent magnetization observed in either curve. The saturation magnetization of Fe_3O_4 nanoparticle-inclusion microcontainers was smaller than that of the naked Fe_3O_4 nanoparticles, which indicates that although the magnetization value was decreased because of the Fe_3O_4 nanoparticles encapsulated in the polymer shell, the inclusion microstructure still preserved superparamagnetic behavior. As a control, we demonstrated that the magnetic hysteresis curve was not obtained for microcontainers without Fe_3O_4 nanoparticle inclusion. Therefore, the superparamagnetic Fe_3O_4 nanoparticles were embedded in the shells of capsules possessing an effective external alternating magnetic field response when under time-varied magnetic field exposure. This enables the shell to change

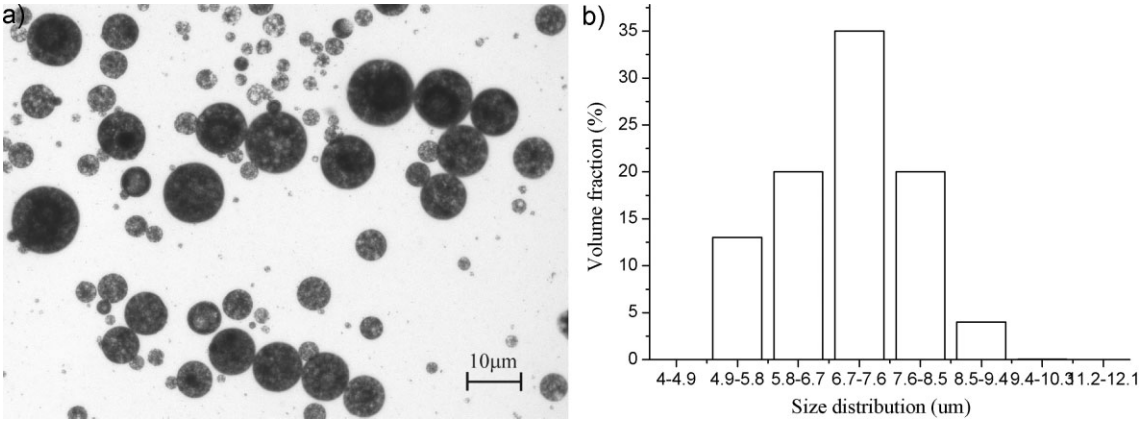

Figure 2. Microscopy image of Fe_3O_4 nanoparticle-inclusion microcontainers in bright fields (a) and their relative size distribution (b). The mean diameter of the microcontainers was 7.26 μm. The intensity scale on the *y* axis represents the volume fraction of each size.

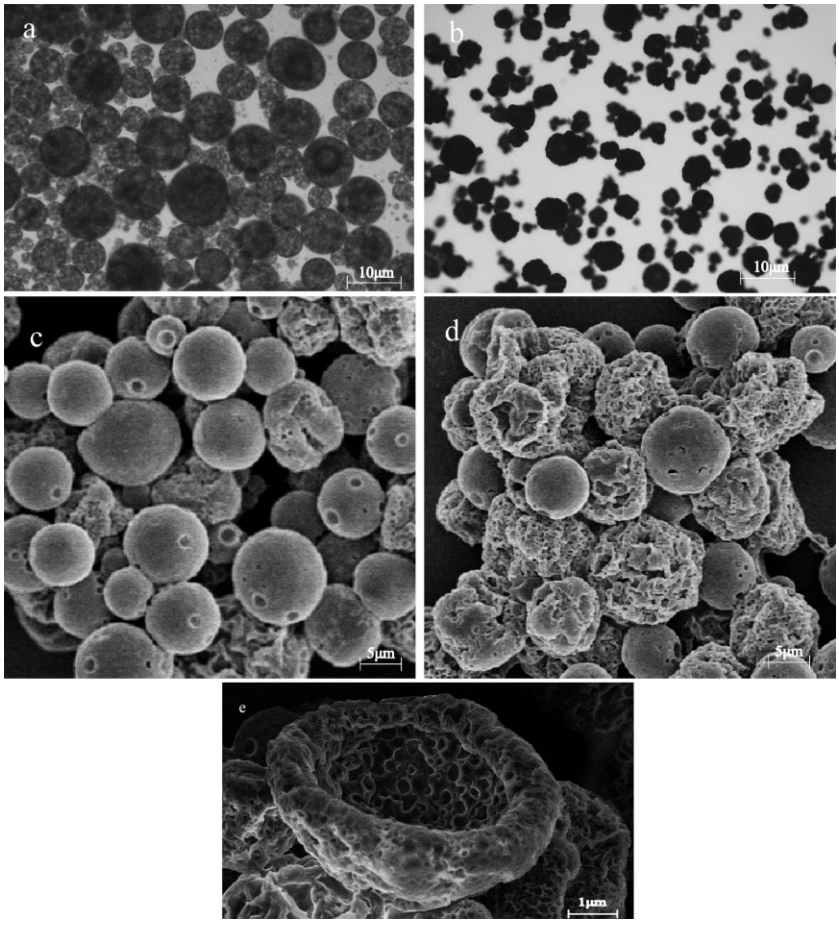

Figure 4. Morphology of Fe_3O_4-inclusion microcapsules. a) Optical microscopy and c) SEM images before treatment with an alternating magnetic field. b) Optical microscopy and d) SEM images immediately after alternating magnetic field treatment. e) SEM image of the damaged microreactors after further ultrasonic exposure.

between a closed and an open state, which turns the microcapsule into a bubble reactor in a controllable way.

To evaluate the effect of the alternating magnetic field on the integrity of the shell of the microcontainers, suspensions of microcontainers in H_2O_2 solution were subjected to treatment with an alternating electromagnetic field of frequency 50 000 Hz and magnetic intensity 80 000 A m^{-1} for 10 min. Figure 4 shows optical microscopy and scanning electron microscopy (SEM) images of the capsules before and after magnetic treatment. The morphology of the capsules is clearly changed after magnetic and ultrasonic field treatment. The images in Figure 4a and c show that the shell surface is relatively smooth and perfect before treatment with the alternating magnetic field. However, after magnetic field treatment, more than 80% of the shell surface of the capsules is rough and there are many dimple-like rumples on the shell (Figure 4b,d). A transient opening state of the shell may be caused by exposure to the alternating magnetic field, which results in the outside solution diffusing almost instantaneously into the capsule interior. After US imaging and further US exposure, the bubble microreactors were broken down, and bubble-hole craters in the inner shell surface topology were observed (Figure 4e) by SEM. The significant morphology change was not found in control samples without the nanoparticles. In light of these results, it is demonstrated that after alternating magnetic treatment the shell permeability can be changed and the microcontainers can be transformed into bubble microreactors.

Figure 5 shows US images obtained before and after alternating magnetic field treatment. Upon exposure of arginine inclusion capsules (0.25 mmol L^{-1}) to H_2O_2 solution (0.25 mmol L^{-1}) under an alternating magnetic field, the enhancement of the shell permeability leads to the entrance of H_2O_2 and arginine can be reduced to NO gas. After washing with distilled water, the NO microreactor can be imaged by a digital B-mode diagnostic ultrasonic instrument. US images were captured of degassed and deionized water and samples before and after magnetic field treatment (see Figure 5a–d). Compared with Figure 5a and b of the degassed and deionized water and the microcapsule solution before magnetic field treatment, respectively, a brighter area can be seen distinctly after exposing the microcontainers to the magnetic treatment. In contrast, the US enhancement of NO bubbles did not occur in the solution of Fe_3O_4 nanoparticle-inclusion microcapsules before magnetic treatment, or in solutions without Fe_3O_4 nanoparticle-inclusion microcapsules before and after magnetic treatment. The US imaging observations and acoustic exposure lasted for 30 min.

To quantitatively measure the change in brightness of the US images, a ''mean gray scale'' was calculated as the average of the gray-scale levels of all pixels within a region of interest (ROI). The image sampled by the imaging system was 8 bits; thus, the range of the pixel gray-scale level was 0–255. Selection of the ROI and calculation of the mean gray scale for each ROI were completed with a purpose-designed MATLAB computer program. For every sample, the images of the three scanned segments were processed, and then the average value of the three mean gray scales of the ROIs was taken as the mean gray scale of the sample. The change curve of the mean gray scales within the ROI is shown in Figure 5e. According to the change in the mean gray scale, we presume that the entrance of H_2O_2 into the capsules is a precursor for the reaction between arginine and H_2O_2. It occurred because the shell permeability was changed upon exposure to the alternating magnetic field. At the beginning, more and more NO gas was gradually generated in the microcontainers, which made the microcontainer an efficient echogenic bubble microreactor and caused the US images to become brighter and brighter. Then, under further US field exposure, the intensive oscillation of NO bubbles in the microreactor destroyed the shell (Figure 4e) and NO gas could be released from the microreactor

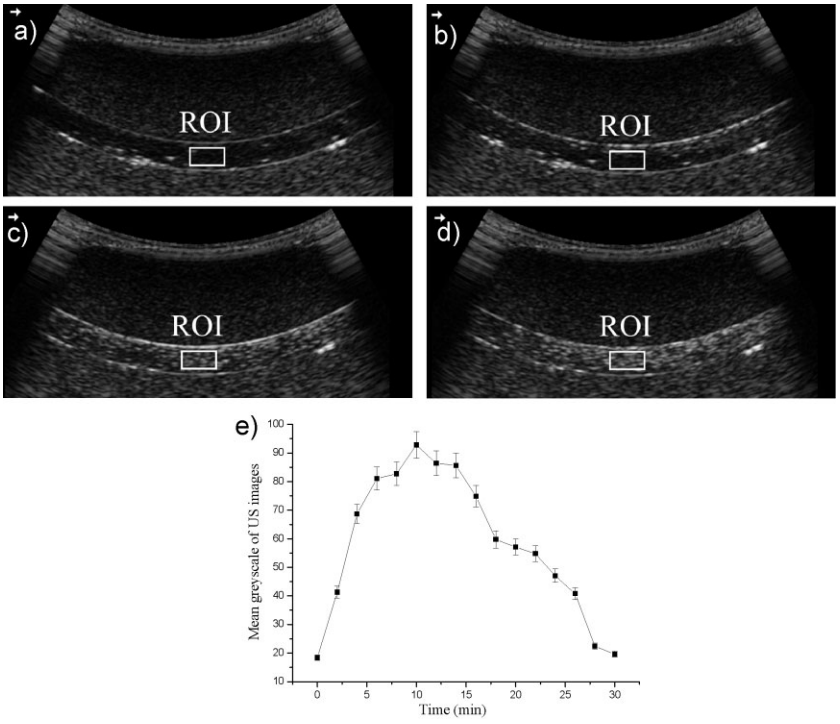

Figure 5. a–d) In vitro US images of the different samples: a) degassed and deionized water; b) the microcontainer solution before alternating magnetic field treatment; c,d) the microcontainer solution after alternating magnetic field treatment when US imaging lasted for 2 and 10 min, respectively. e) After magnetic field treatment, the mean gray scale of the US images was captured. The enhancement of the US imaging changed over time.

to dissolve into the outside solution. Therefore, after about 12 min, the US contrast enhancement efficiency became poorer and poorer until the mean gray scale of the US images was just like that at the beginning. However, at this moment, although the US imaging enhancement effect of the NO bubbles disappeared because they were released and readily diffused into the outside solution, the free dissolved NO could be a useful therapeutic agent.

It is well known that NO gas plays an important role in many relevant bioprocesses, from controlling arterial thrombosis to endothelium regeneration, antithrombotic activity, and in cardiovascular diseases by inhibiting the platelet aggregation process.[22,23] Control of the release of NO gas in the disease site is beneficial for the above diseases. The microcontainers fabricated in this work are intelligent, externally triggered microstructures. By controlling the modulation of the arginine–NO pathway through alternating magnetic and acoustic field exposure, the Fe_3O_4 nanoparticle-inclusion microcontainers showed a satisfactorily controlled release feature. Therefore, they can be used in a broad range of diagnostic and therapeutic applications, including US imaging and NO therapy.

In fact, according to the choice of coating material, macromolecular therapeutics can be encapsulated inside these microcapsules or microcontainers. Their mechanical strength can be tailored by varying the number of coating layers, inclusion of nanoparticles, or by thermal treatment.[24] In particular, nanoparticles can be embedded in the walls of the capsules not only to change the viscoelastic characteristics of the microcapsule shell, but also to provide biological functionality.[25] Experimental results show that, at comparable diameters, the effective permeability of shells doped with Fe_3O_4 nanoparticles is very different from the permeability of control samples without nanoparticles.

Two facts indicate the possible mechanism and driving force that causes the permeability changes. First, some experimental studies have shown that colloidal particles or nanoparticles embedded in the shell can change the mechanical or optical properties of the shell, because nanoparticles may influence the bending elasticity of the membrane.[26,27] Therefore, nanoparticles embedded in the shell have the potential to change the shell properties and hence alter the permeability property of the shells.[28] Second, it is generally understood that the presence of superparamagnetic Fe_3O_4 nanoparticles within the polymer membrane can offer a magnetic-field-triggered stimulus response effect that allows self-stirring of the microcontainers under the alternating magnetic field. The movement of Fe_3O_4 nanoparticles in the shell weakens the polymer binding. The nanoparticles were therefore rearranged in the shell and enhanced the permeability, which allowed the H_2O_2 outside and arginine inside to diffuse into each other via transient polymer breaking and reestablishment. Although the exact mechanism of this process has remained, until now, obscure, bubble generation in the microcapsules that enhances the US imaging and the steplike change of the mean gray scale of the US images all favor the hypothesis of a strong influence of Fe_3O_4 nanoparticle redistribution upon weakening the polymer interactions, and the subsequent increased diffusion of the agents inside and outside of the microcontainers. Once the bubbles are produced in the microreactor, the acoustic characteristic of the bubbles can change the microcontainers into US imaging bubble microreactors. Further acoustic exposure would allow the NO released into the microenvironment to act with a therapeutic function.[29,30] Of course, for the use of these systems as controlled-delivery bubble microreactor devices, there are still significant challenges remaining to make the microcontainers into a bubble microreactor system with easy remote control and accurate release.

In summary, we have demonstrated that microcontainers with embedded superparamagnetic Fe_3O_4 nanoparticles can be changed into bubble microreactors after treatment with an alternating magnetic field. This elaborately fabricated microstructure can realize the combination of US diagnostic and NO therapeutic multifunctionalities. It is envisioned that magnetic-field-triggered permeability could become a very easy, important, and effective way to fabricate diagnostic and therapeutic microdevices.

Experimental Section

Materials: Poly(D,L-lactide) (PLA; $M_w = 10\,000$) was purchased from Shandong Key Laboratory of Medical Polymer Materials. Poly(vinyl alcohol) (PVA), 88 mol% hydrolyzed with a M_w of 25 000, was from Sigma–Aldrich. L-Arginine was purchased from Beyotime Institute of Biotechnology (Haimen, China). Superparamagnetic iron oxide (SPIO; Fe_3O_4) with a mean diameter of 12 nm was from Jiangsu Laboratory for Biomaterials and Devices.[31] H_2O_2 was purchased from Sinopharm Chemical Reagent Co., Ltd (Shanghai, China). Span 80 and Tween 80 were reagent grade.

Fabrication of microemulsions: The microcontainers were prepared by the double-emulsion method. Briefly, a methylene chloride solution (10.00 mL) was prepared containing PLA (0.50 g) and hydrophobic Fe_3O_4 nanoparticles (0.20 g) at 25 °C. To generate the first water-in-oil (W/O) emulsion, L-arginine solution (2.00 mL, 0.25 mmol L^{-1}) and Tween 80 (about 0.05 mL) were added to the organic solution and sonicated continuously by a US probe at 200 W for 2 min. This W/O emulsion, which was brown and visibly homogeneous, was then poured into a 5% PVA (w/v) solution (30.00 mL) and mixed mechanically for 2 h to form a (W/O)/W stable multiple emulsion. After reaction, the final emulsion became milk-white.

Vibrating-sample magnetometry: The magnetization property at room temperature (20 °C) of the Fe_3O_4-inclusion microcapsules was studied by using a 7407 vibrating-sample magnetometer (Lake Shore Cryotronics, Inc, OH, USA). The samples included the naked Fe_3O_4 nanoparticles and Fe_3O_4-inclusion microcontainers. The latter samples were dried by spray drying prior to analysis (Buchi B-290, Switzerland). Due to the relatively low magnetic moment of the samples, the correct hysteresis loops were obtained after subtracting the offset background signals. Saturation magnetization, coercive force, and remanent magnetization were obtained from the hysteresis loops. Each sample was measured in triplicate.

Magnetic field treatment: An alternating electromagnetic field, with frequency of 50 000 Hz and a magnetic intensity of 80 000 A m^{-1}, was applied to oscillate and disturb the Fe_3O_4 nanoparticles embedded in the microcapsule shells. Immediately after mixing the magnetic microcontainers (3 mL) and H_2O_2 solution (2 mL, 0.25 mmol L^{-1}), the mixture was kept inside the alternating magnetic field for 10 min before checking the shell permeability. Immediately after magnetic treatment, the H_2O_2 solution was replaced by deionized water through centrifugal separation. US imaging was selected as an effective verification means for the NO bubbles produced in the microcontainers.

US imaging and ultrasonic treatment: An in vitro US imaging test was used to verify the presence of the generated bubbles in the microcontainers after an alternating magnetic field was applied. If the H_2O_2 solution can enter into the shell of the microcontainer, the arginine can be reduced by the H_2O_2 solution into NO gas. The free NO gas in the microcontainers can then be imaged by US imaging. The images of the microcontainer solution before and after magnetic field treatment were obtained by a digital B-mode diagnostic ultrasonic instrument (Belson3000A; Belson Imaging Technology Co., Ltd., Wu Xi, China) with a 3.5 MHz R60 convex-array probe. The images were stored every 1 min within the observation period. Then the ROI was located within the pipeline in the phantom excluding the walls of the channel, and the average pixel intensity of the ROI was calculated. The measurements of all samples were repeated three times.

Characterization: Samples in solution were placed between glass slides and observed with an Axioskop 40 microscope equipped with a Coolsnap MP3.3 camera (Carl Zeiss, Germany). For SEM (Hitachi S-4800, Japan) analysis, a drop of each sample solution was applied to a $1 \times 1\ cm^2$ silicon wafer with sequential drying. The samples included microcontainer solutions before and after application of alternating magnetic fields.

Keywords:

diagnostics · drug delivery · magnetic materials · microreactors · nanoparticles

[1] J. Kim, Y. Piao, T. Hyeon, *Chem. Soc. Rev.* **2009**, *38*, 372.
[2] M. Caldorera-Moore, N. A. Peppas, *Adv. Drug Delivery Rev.* **2009**, *61*, 1391.
[3] X. J. Ju, R. Xie, L. Yang, L. Y. Chu, *Expert Opin. Ther. Pat.* **2009**, *19*, 683.
[4] G. Ibarz, L. Dähne, E. Donath, E. Donath, H. Möhwald, *Adv. Mater.* **2001**, *13*, 1324.
[5] M. Matsusaki, M. Akashi, *Expert Opin. Drug Delivery* **2009**, *6*, 1207.
[6] S. H. Hu, C. H. Tsai, C. F. Liao, D. M. Liu, S. Y. Chen, *Langmuir* **2008**, *24*, 11811.
[7] M. F. Bédard, D. Braun, G. B. Sukhorukov, A. G. Skirtach, *ACS Nano* **2008**, *2*, 1807.
[8] A. G. Skirtach, A. M. Javier, O. Kreft, K. Kohler, A. P. Alberola, H. Mohwald, W. J. Parak, G. B. Sukhorukov, *Angew. Chem.* **2006**, *118*, 4728; *Angew. Chem. Int. Ed.* 2006, *45*, 4612.
[9] B. G. De Geest, A. G. Skirtach, A. A. Mamedov, A. A. Antipov, N. A. Kotov, S. C. De Smedt, G. B. Sukhorukov, *Small* **2007**, *3*, 804.
[10] X. J. Ju, R. Xie, L. Yang, L. Y. Chu, *Expert Opin. Ther. Pat.* **2009**, *19*, 493.
[11] L. Y. Chu, T. Yamaguchi, S. Nakao, *Adv. Mater.* **2002**, *14*, 386.
[12] T. Hoare, J. Santamaria, G. F. Goya, S. Irusta, D. Lin, S. Lau, R. Padera, R. Langer, D. S. Kohane, *Nano Lett.* **2009**, *9*, 3651.
[13] W. C. Huang, S. H. Hu, K. H. Liu, S. Y. Chen, D. M. Liu, *J. Controlled Release* **2009**, *139*, 221.
[14] S. H. Hu, K. T. Kuo, W. L. Tung, D. M. Liu, S. Y. Chen, *Adv. Funct. Mater.* **2009**, *19*, 3396.
[15] S. H. Hu, S. Y. Chen, D. M. Liu, C. S. Hsiao, *Adv. Mater.* **2008**, *20*, 2690.
[16] S. H. Hu, T. Y. Liu, H. Y. Huang, D. M. Liu, S. Y. Chen, *Langmuir* **2008**, *24*, 239.
[17] V. Petrovića, B. Buzadžića, A. Koraćb, A. Vasilijevića, A. Jankovića, B. Korać, *Chem. –Biol. Interact.* **2009**, *182*, 204.
[18] G. Wu, T. E. Haynes, H. Li, W. Yan, C. J. Meininger, *Biochem. J.* **2001**, *353*, 245.
[19] L. I. Filippin, A. J. Moreira, N. P. Marroni, R. M. Xavier, *Nitric Oxide* **2009**, *21*, 157.
[20] E. Stride, K. Pancholi, M. J. Edirisinghe, S. Samarasinghe, *J. R. Soc. Interface* **2008**, *5*, 807.
[21] J. Wu, W. L. Nyborg, *Adv. Drug Delivery Rev.* **2008**, *60*, 1103.
[22] W. S. Jobgen, S. K. Fried, W. J. Fu, C. J. Meininger, G. Wu, *J. Nutr. Biochem.* **2006**, *17*, 571.
[23] D. Ralt, *Med. Hypotheses* **2009**, *73*, 794.
[24] C. S. Peyratout, L. Dähne, *Angew. Chem.* **2004**, *116*, 3850; *Angew. Chem. Int. Ed.* 2004, *43*, 3762.
[25] O. B. Usta, A. Alexeev, G. Zhu, A. C. Balazs, *ACS Nano* **2008**, *2*, 471.
[26] M. Abkarian, A. B. Subramaniam, S. H. Kim, R. J. Larsen, S. M. Yang, H. A. Stone, *Phys. Rev. Lett.* **2007**, *99*, 188301–1.

[27] L. Hoff, P. C. Sontum, J. M. Hovem, *J. Acoustics Soc. Am.* **2000**, *107*, 2272.
[28] F. Dubreuil, D. G. Shchukin, G. B. Sukhorukov, A. Fery, *Macromol. Rapid Commun.* **2004**, *25*, 1078.
[29] M. Postema, A. Bouakaz, F. J. ten Cate, G. Schmitz, N. de Jong, A. van Wamel, *Ultrasonics* **2006**, *44*, e109.
[30] D. G. Shchukin, D. A. Gorin, H. Möhwald, *Langmuir* **2006**, *22*, 7400.
[31] Z. Chen, Y. Zhang, S. Zhang, J. Xia, J. Liu, K. Xu, N. Gu, *Colloid Surf. A* **2008**, *316*, 210.

Received: February 3, 2010
Revised: March 29, 2010
Published online: May 19, 2010

